DIAMANTI
3D-PRINTED, POST-TENSIONED CONCRETE CANOPY

MASOUD AKBARZADEH / HUA CHAI / YEFAN ZHI / MAXIMILIAN E. ORORBIA / TENG TENG
UNIVERSITY OF PENNSYLVANIA - POLYHEDRAL STRUCTURES LAB (PSL)
MATHIAS BERNHARD
ÉCOLE POLYTECHNIQUE FÉDÉRALE DE LAUSANNE (EPFL)
DAMON (MOHAMMAD) BOLHASSANI / FAHIMEH YAVARTANOO / JAVIER TAPIA
THE CITY COLLEGE OF NEW YORK (CCNY)
KAROLINA PAJAK / MYLÈNE BERNARD / LEON TROUSSET
SIKA CORPORATION
PAUL KASSABIAN / BLAISE WALIGUN
SIMPSON GUMPERTZ & HEGER (SGH)

This academia–industry collaborative project, *Diamanti canopy*, demonstrates the design and fabrication of a combined compression and tension funicular canopy with periodic anticlastic, diamond surfaces (Fig. 3).
The canopy is a part of the European Cultural Centre's 2024 biennial exhibition, 'Personal Structures', in Venice, Italy, at the Giardini della Marinaressa (Fig. 2). Utilising both 3D concrete printing (3DCP) and post-tensioning technologies, the canopy spans 10m and is supported by a cross-laminated timber (CLT) platform (Fig. 4).
The structural form of this composite canopy directly considers both compressive and tensile forces, inherently developed in concrete structural systems, by distributing loads through its unique, minimal-mass geometry.
The CLT platform suggests how the combination of a carbon-negative material and concrete can be used in contrast to common construction methods where concrete is typically used as the load-bearing support and wood as the spanning element. Hence, the lightweight design of the *Diamanti canopy*, spanning over and supported by the CLT platform, showcases the innovative use of these materials, while also satisfying the Venice Port Authority's installation requirements.

The historical design of ancient masonry structures continues to inspire the use of compression-dominant structures in the Architectural, Engineering, and Construction (AEC) sector because of their ability to perform well and minimise the amount of material, mass, and embodied energy required (López López *et al.*, 2014, and Nuh *et al.*, 2022). While beneficially reducing the overall quantity of material needed for construction, such systems call for extensive external provisions to maintain compression-only load paths requiring, for example, either fixed boundary conditions or the inclusion of horizontal tension-ties as constraints. Other safety requirements may necessitate the inclusion of additional reinforcement, such as steel fibres, to enhance performance, but can limit the structure's ability to be recycled.

The exhibited canopy goes beyond compression only by embracing tension as an unavoidable force in systems resilient to different loading scenarios. Hence, a combined form-finding and fabrication approach was developed to achieve the innovative structure with the intention of also minimising carbon through reduced materials and recyclability. Through the design freedom enabled by the design approach, 3DCP, and the use of post-tensioning, the final design favourably has minimal reinforcement

1

2

while achieving the desired structural performance. Overall, the *Diamanti canopy* demonstrates how, through the combination of modern technologies and the development of a non-restrictive, comprehensive design approach, new structural forms can be achieved that lead to enhanced sustainable practices.

The geometry-based structural design method of polyhedral graphic statics (PGS) (Akbarzadeh, 2016; Lee, 2018) provided the design freedom to achieve a structure that is capable of dealing with developed compression and tension forces. Polyhedral cells, defined from the resulting structural form, were used to contort periodic anticlastic surfaces, specifically the diamond triply periodic minimal surface (TPMS) geometry to align with the principal stress directions. The diamond TPMS unit's geometry enhances the structural form's geometric stiffness and inherently provides the internal conduits for the post-tensioned cables, resulting in a fully integrated material-structural system.

The use of 3D concrete printing allowed for the effective realisation of the innovative structural form, which otherwise could not be achieved using standard construction techniques. Prefabrication optimisation and construction schemes were developed to address additive manufacturing constraints. To optimise for printability, signed distance function (SDF) (Bernhard *et al.*, 2018; Blinn, 1982; Bernard *et al.*, 2021) combined the funicular form and the TPMS geometry into a smooth, unified model. To print the 10m canopy, the design was divided into segments that ensured preferred structural behaviour and optimisation algorithms were developed to effectively slice the segmented geometry with non-parallel planes perpendicular to the direction of compression force flow. Additional computational algorithms were developed for efficient non-continuous printing to minimise the material dripping and to avoid collision, since the geometry of the segments includes multiple disconnected loops.

3

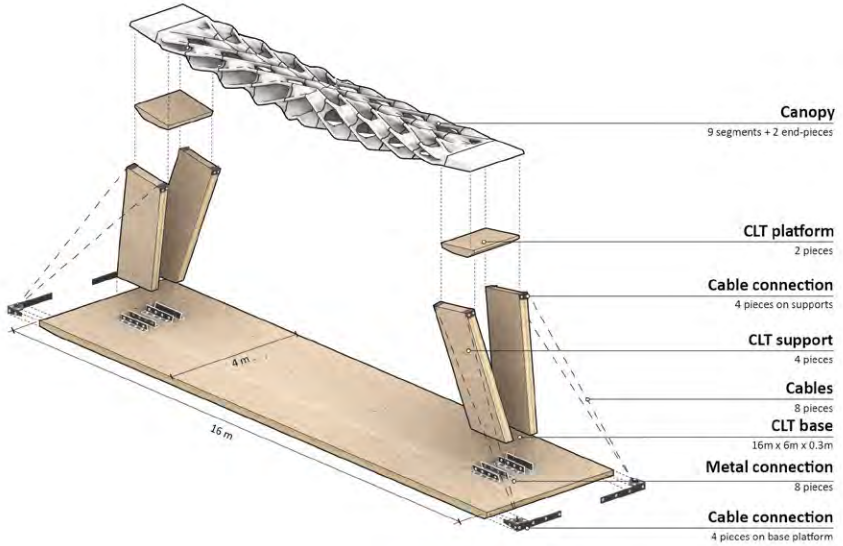

4

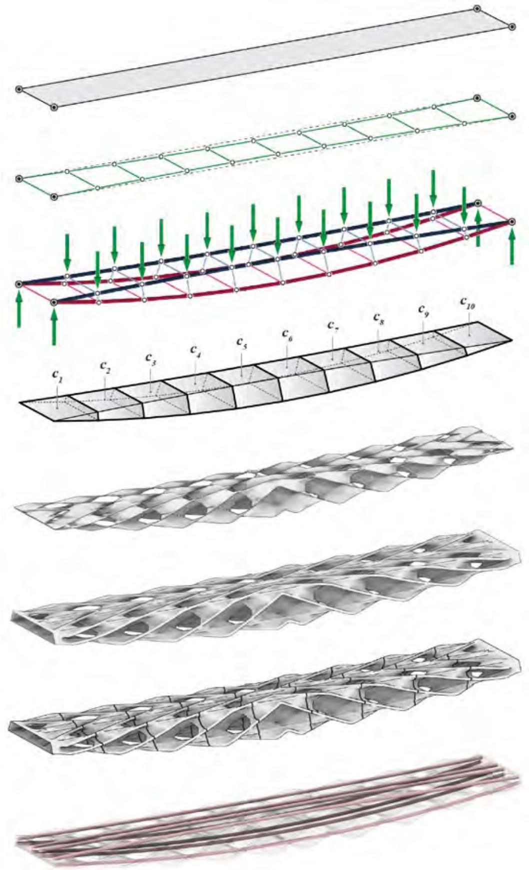

1. 1:10-scale clay model fabricated using the in-house modular printer. © Polyhedral Structures Lab, University of Pennsylvania.

2. Rendering of canopy at the Giardini della Marinaressa, Venice, Italy: © Polyhedral Structures Lab, University of Pennsylvania.

3. 3D concrete printed periodic anticlastic funicular canopy. © Polyhedral Structures Lab, University of Pennsylvania.

4. Assembly concept of canopy exhibition. © Polyhedral Structures Lab, University of Pennsylvania.

5. Structural form-finding through polyhedral graphic statics and volumetric modelling. © Polyhedral Structures Lab, University of Pennsylvania.

5

The overall design and fabrication approach in this work includes multiple intertwined innovative strategies that result in an extremely efficient structural system utilising 3D concrete printing and post-tensioning that reduces the construction materials needed compared with conventional structural systems. The prefabrication strategy yields faster erection times, reduces soft construction costs, eliminates the need for formwork, allows for recyclability, and minimises the overall carbon emissions of concrete construction.

Design

A comprehensive computational methodology for form-finding, optimisation, and digital fabrication was developed to design the canopy. The method begins with the generation of a geometric design using PGS, succeeded by the utilisation of volumetric modelling (VM) for structural materialisation. With respect to fabrication, details concerning 3DCP were considered through the development of print-specific optimisation algorithms. The entire computational method for the canopy is illustrated as a workflow in Fig. 5. While applied here to the canopy, this computational method is general in that the process from design generation to digital fabrication preparation can be employed for a wide range of applications. The specifics of the method are discussed subsequently.

Structural form-finding through polyhedral graphic statics

The structural form-finding process begins with the implementation of graphic statics. Conventional two-dimensional graphic statics establish a reciprocal relationship between form and force. This reciprocity principle allows for the considered forces and form to be altered without violating structural equilibrium, providing design freedom. With stability guaranteed, a range of stable structural forms can be generated considering both tension and compression forces (Fig. 6a). To effectively manage design requirements and material properties for the concrete canopy design, it is beneficial to maintain constant tension forces. In the context of 3D printing,

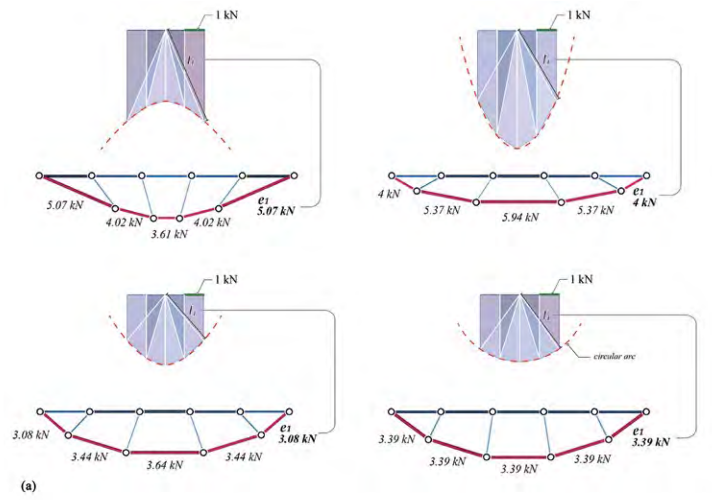

6

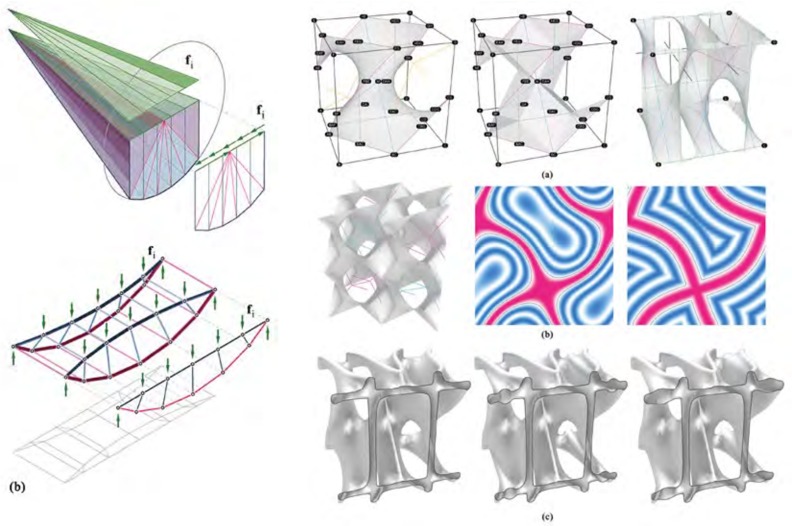

7

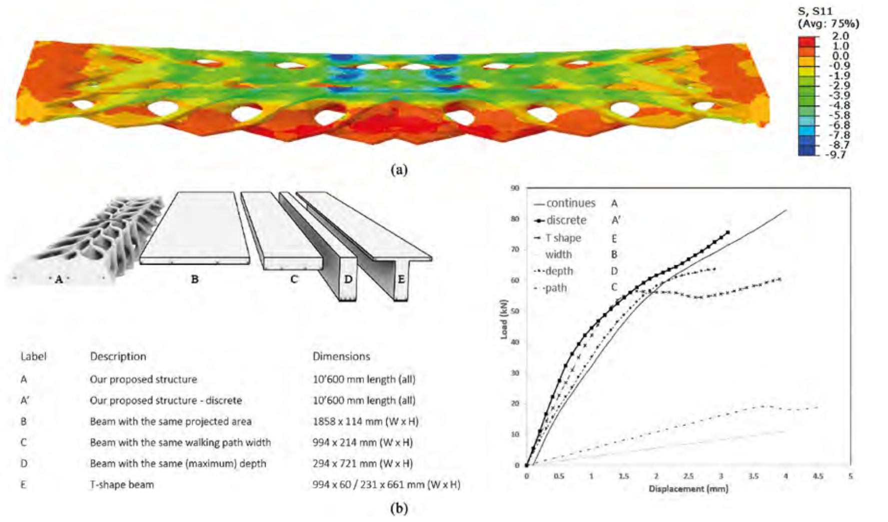

8

concrete materials exhibit anisotropic behaviour, meaning their properties vary depending on the direction of the applied load. The final constant tension force determined from graphic statics can be used as the post-tensioning force for the cables that run through the canopy to ideally produce constant compression. While the constant compression force intended to be developed from post-tensioning the system reduces the risk of localised stress concentrations and delamination of printed layers, the steel post-tensioning strands provide necessary steel reinforcement, allowing for the canopy to deal with tension forces that could be developed from other loading scenarios.

After using two-dimensional graphic statics to determine a geometry capable of dealing with combined tension and compression forces, PGS is utilised to extend the form and force in the third dimension (Fig. 6b). For this project, all the edges defining the two-dimensional force diagram are extruded to two points to establish a new three-dimensional force diagram. The same strategy used in two-dimensional graphic statics to ensure constant tension forces is also applied here. With the form established, segmented cells are defined to be used later for materialisation and VM of the anticlastic surfaces.

Embedding periodic anticlastic surfaces

Since first described by Hermann Amandus Schwarz (1865), and later by Edvard Rudolf Neovius, Alan Hugh Schoen, and others, periodic anticlastic surfaces, specifically TPMS, are studied in several domains, including mathematics, physics, material science, engineering, and architecture to name a few.

A surface is defined as anticlastic when the centres of curvatures are located on opposing sides, forming a hyperbolic paraboloid. The intricate structure of periodic anticlastic surfaces, their high surface-to-volume ratio, and their property of separating space into two interwoven but disconnected sub-spaces, make them promising candidates for a variety of applications, including, for example, medical implants, lightweight infill structures, and heat exchangers. While the gyroid surface, discovered by Schoen, is commonly the focus of various applications, the Schwarz-D TPMS, also named 'Diamond' by Schoen, is implemented here for the canopy's design because of its diamond cubic labyrinths. The diamond surface can be approximated by the implicit function:

$$\cos x \cos y \cos z - \sin x \sin y \sin z = 0$$

The surface is the 0-level isosurface of this function, separating space in a positive and a negative half-space. Unlike the gyroid, the diamond has several straight lines embedded in its surface that can be separated into three sets (Fig. 7a). A series of transformations are applied to rotate, translate, scale, and mirror the initial unit characteristics to align with the geometry generated through PGS. While different alignments can be explored, the continuity of the smooth surface must be guaranteed by enforcing the wavelength to be an integer multiple of 1 when cells are lined up and morphed into the form diagram, as done with the canopy illustrated in Fig. 5.

While the smooth zero mean curvature of minimal surfaces is beneficial in some applications, it poses some interesting challenges when 3D printed in concrete. The shallow horizontal parts of the surface at the saddle

6. Force and form diagrams of the geometry generated using a) graphic statics, and b) polyhedral graphic statics. © Polyhedral Structures Lab, University of Pennsylvania.

7. Periodic anticlastic surface and volume generation: a) diamond unit cell and approximated polyhedral surface; b) rhombi structures revealed by red and blue labyrinths; and c) thickened diamond surfaces with blended cavities. © École Polytechnique Fédérale de Lausanne.

8. Finite element modelling and analysis, and comparison with other beam structures. © City College of New York.

points constitute large overhangs that lead to printing in mid-air or can lead to structural collapse. To overcome this challenge, the implicit surface was replaced by a topologically identical polyhedral version (Fig. 7a), which natively contains angles acute enough to be readily printed. This polyhedral simplification (Fig. 7a) embraces the stunning relation between the labyrinths (Akbari *et al.*, 2021), Laves graphs, and VM with distance functions, whereby the diamond surface is equally distant from both labyrinths (i.e., continuous interwoven Voronoi cells), and appears to be made of planar rhombi (Fig. 7b).

Volumetric modelling

The 0-level isosurface of an implicit function – for example, an SDF – delimits the positive from the negative subspace: everything negative is considered inside the object, and everything positive outside. To materialise the surface itself, the object needs to be defined with an 'inside' and 'outside'. A straightforward way to achieve this is by creating a shell SDF in the form, where *v* is the original distance value and *d* is the desired thickness of the shell. This strategy works well for exact distance functions that exist for many primitives (Bernhard *et al.*, 2018). However, since TPMS are approximated using trigonometric functions, their return values do not reflect actual correct metric distances (Fig. 7b). Applying the shell function does not result in a constant thickness offset of the original surface. The cells in the form diagram vary significantly in size and the same value for *d* would result in very different thicknesses of the shell along the canopy. Additionally, 3DCP requires the contour to be equally spaced – if the surfaces are too close then the extruded material overlaps and collides, diminishing the visual quality; if too far apart, the material does not bond, thereby diminishing the structural integrity. Therefore, a multi-step translation is applied between volumetric and mesh modelling. The polyhedral simplified unit cell single surface is deformed, preserving its topology such that it aligns the unit cube with the hexahedral cells of the form diagram (Fig. 5, step 5). The mesh for each quadrant of the canopy is converted into a distance field to allow for an exact offset (Fig .7b).

The straight lines embedded in the surface align and are perpendicular with the main canopy's thrust lines – that is, the locations where tension and compression forces develop (Fig. 7a). This embedment allows a direct transfer of compression forces without buckling the doubly curved surface. Since the canopy will experience tensile forces in its lower regions, cavities for post-tensioning steel cables are integrated in the canopy's final design by locally dilating the opposite contours (print paths) of the initial shell. Capsules are created along each cable segment and united with the shell (Fig. 7c). With conventional boundary representation modelling, both thickening the mesh by a constant offset and the union of it with more objects would be prone to failure. Beneficially with VM, shapes are computed rather than constructed and the Boolean union computations are effortless. While a strict union leads to hard edges where the objects intersect, both slowing down the printing and being aesthetically displeasing, a smooth union is performed based on exponential functions (Bernhard *et al.*, 2018), which instead seamlessly blends the cylinders into the shell (Fig. 7c).

Numerical and experimental analysis

To understand the structural performance of the canopy, a finite element model was developed and analysed (Fig. 8a). Considering different loads, such as self-weight and service loads, the finite element analyses indicate that the canopy's displacement is significantly less than the maximum displacement limit established by the American Association of State Highway and Transportation Officials (AASHTO, 2008) design guidelines for spanning structures. A further study was conducted to understand the overall efficiency of the canopy compared with other common structural components that span similar distances. While the canopy initially shows a 14% strength reduction compared with the T-shape beam, by increasing the displacement, all the beams experience plastic deformation, while the canopy favourably shows elastic behaviour. The performance of the canopy compared with other common structural components with the same boundary conditions, the position of reinforcement, the volume of concrete, and an applied displacement on the mid-span, are shown in Fig. 8b. To validate the numerical analyses, several physical models and experimental programs were developed to investigate the structural performance of the canopy. Scaled and full-scale canopies were printed, and their structural performance studied using physical load tests to characterise the properties of the 3D-printed concrete post-tensioned parts and match the analytical results of the finite element analysis with the observed behaviour. These tests led to the development of post-tensioning strategies and techniques to further minimise needed reinforcement and ensure recyclability.

Fabrication

To actualise the designed canopy, both 3D concrete printing and post-tensioning technologies were utilised. Unlike traditional concrete structures, no formwork is needed for the canopy and, indeed, could not be used because of the complexity of the canopy's form. Hence, a multi-component, accelerated 3D concrete printing system was used to print the canopy. The canopy was divided into nine segments, since, at 12m, it would not be feasible to print the canopy all at once. The segments are combined by threading steel cables, 'tying' all segments together, and then compressed when post-tensioned. The assembled canopy is elevated and placed on CLT columns attached to a base for display. The display setup (Fig. 4) was devised with consideration of the soil profile of the Giardini della Marinaressa in Venice and to best exhibit the canopy.

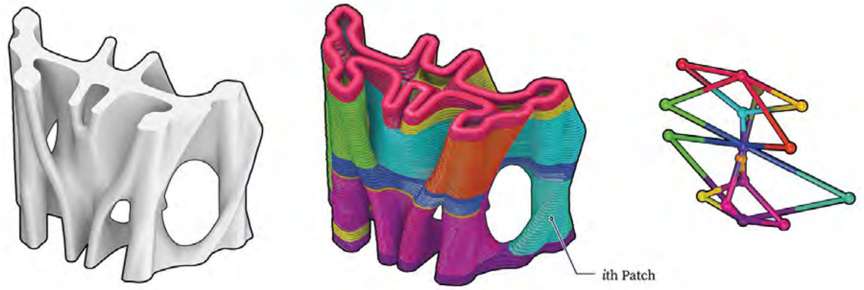

9

To ensure successful print and assembly, models of the canopy at four different scales, 1:10, 3:10, 1:2 (Fig. 10), and 1:1, were produced. The 1:10 scale model was printed to understand the nuances of the canopy's structural form using an in-house-developed desktop 3-axis clay printer, featuring a modularised compressive hopper and an auger-embedded extruder, and assembled by post-tensioning steel strands (Fig. 1). The assembly process of the 1:10 scale model was conducted using an upside assembly procedure. As a high-fidelity proof-of-concept, 3m, half-scaled, and full-scaled versions of the canopy were printed using the multi-component, accelerated 3D concrete printing system, to best understand the printing process and the feasibility of assembly (Fig. 12). Overall, this prototyping informed needed printing procedures and assembly schemes on how to best digitally and physically fabricate and construct the full-scale canopy.

10

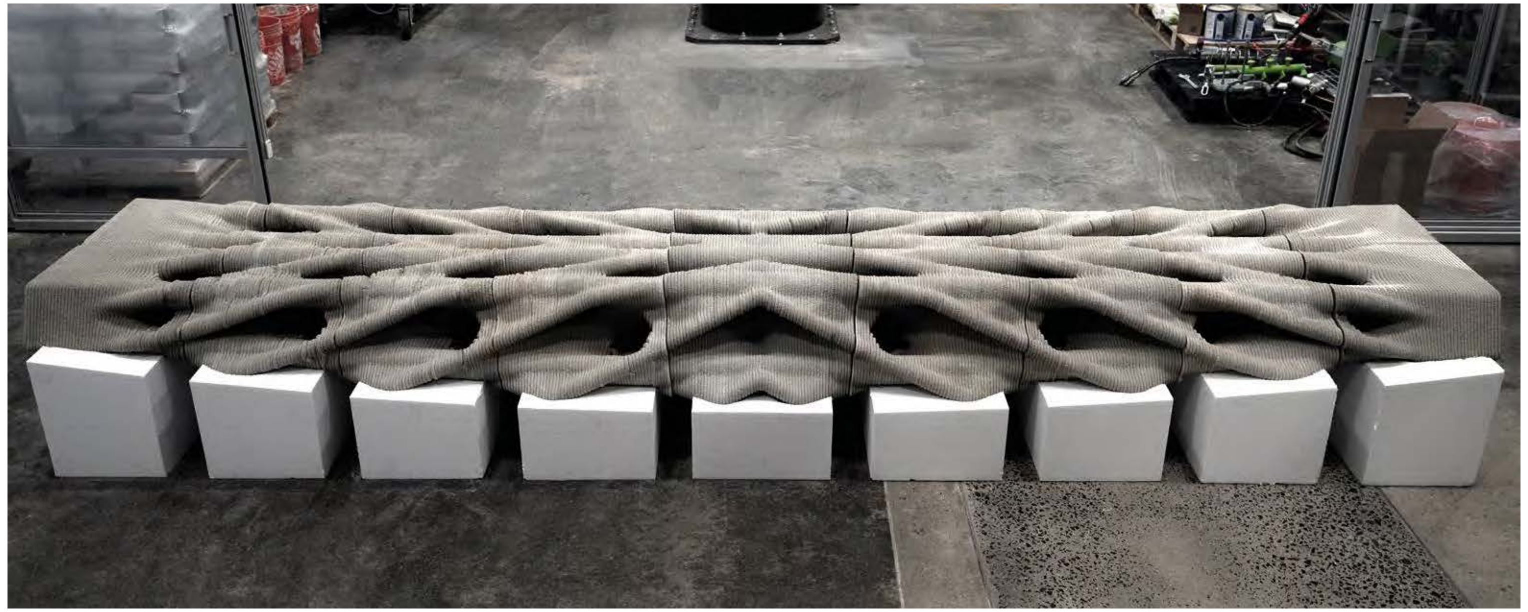

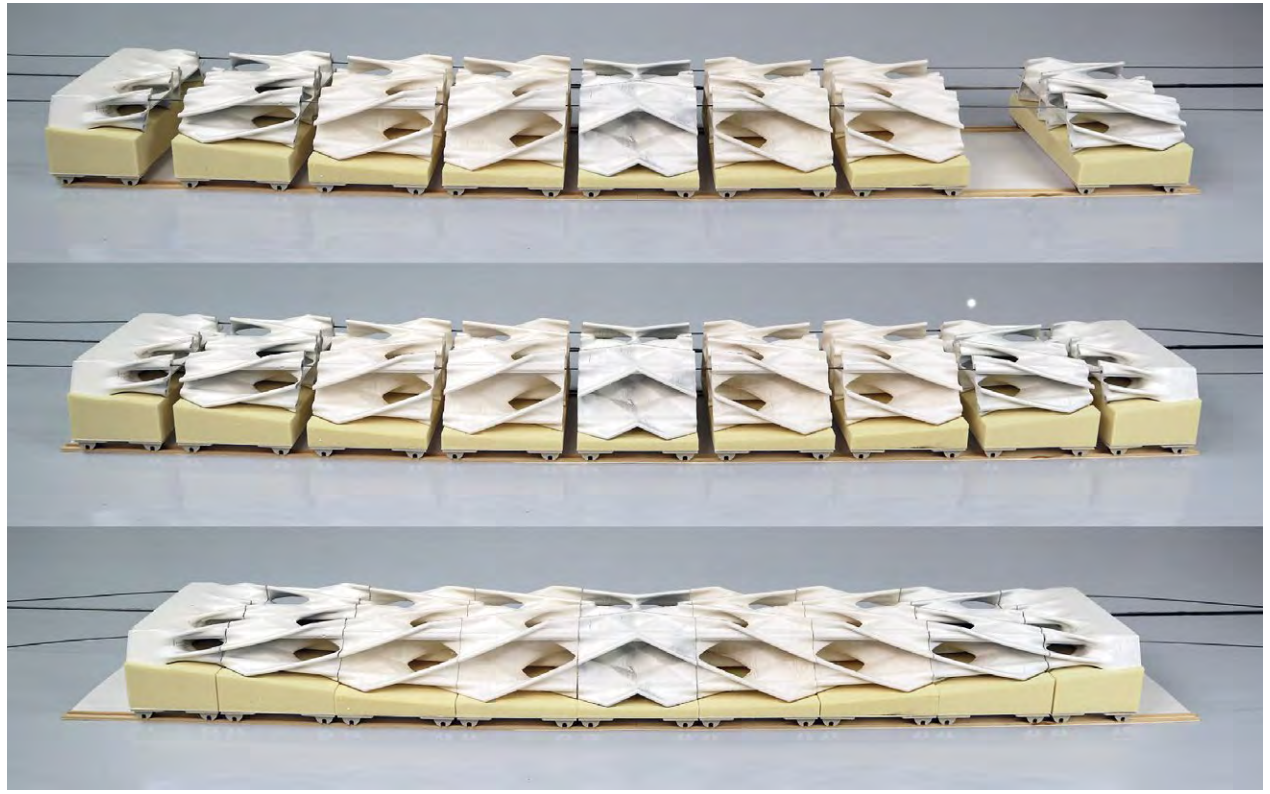

11

9. Continuous toolpath patches generated utilising a dependency graph. © Polyhedral Structures Lab, University of Pennsylvania.

10. 1:2 scale (5m) 3D concrete printed canopy. © Polyhedral Structures Lab, University of Pennsylvania.

11. Machined foam, caster, rail system for assembly and post-tensioning. © Polyhedral Structures Lab, University of Pennsylvania.

Slicing and toolpath generation

Due to the complexity of the canopy's design and the limitations of the large-scale 3D concrete printer, the slicing and final toolpath were adapted to fit this specific process. Non-parallel slicing was used to get the layers perpendicular to the direction of compression forces, brought about by self-weight, during printing. To 3D print non-parallel layers, the printing parameters were adapted to keep the layer width constant. Because of the different inclinations of the layers, the resulting layer heights vary throughout the layer around an average value set to 10mm. Varying layer heights combined with a constant printing speed and extrusion rate create variations in the layer width, around an average set to 30mm. To avoid these layer width variations, an adaptation of the printing speed was implemented based on an algorithm that determines the specific layer height on each point of the toolpath. In case the layer height is lower than 10mm, the printing speed is proportionally increased within the GCode (printing code) to compensate for the layer height variation and keep the layer width of 30mm, and vice versa.

One of the limitations when 3D printing is overhang – that is, parts of the print that slope outwards without support. When the overhang is too high, either the contact surface between the layers is too low to enable further layers to be deposited on top, or the material does not support the structure's self-weight before setting, and parts of the print collapse. Overhangs can be detected during the slicing process by extracting the normal vectors to the mesh model on each face, enabling easier refinement of the shape without creating waste through physical 3D-printing trials. Overall, a goal of reducing overhangs below 35° to maximise the success rate of the print was set.

In addition, since the canopy has hollow sections, it could not be printed in one continuous path. Hence, a few layers were printed at once, and then a 'jump' was made to print the next group of layers. To avoid material dripping during jumps, the material extrusion was halted; however, prolonged stops can potentially lead to the printer nozzle clogging. To reduce the risk of clogs, which are more likely to occur if the extrusion is stopped for more than 2.5 seconds, the printing path was optimised to ensure jumps would occur outside of the printing area, preventing the dripping of excess material on the 3D-printed element. The convex hull of the toolpath was generated to obtain the contour curve of the element; then, for each jump, the contour was duplicated and moved to the respective

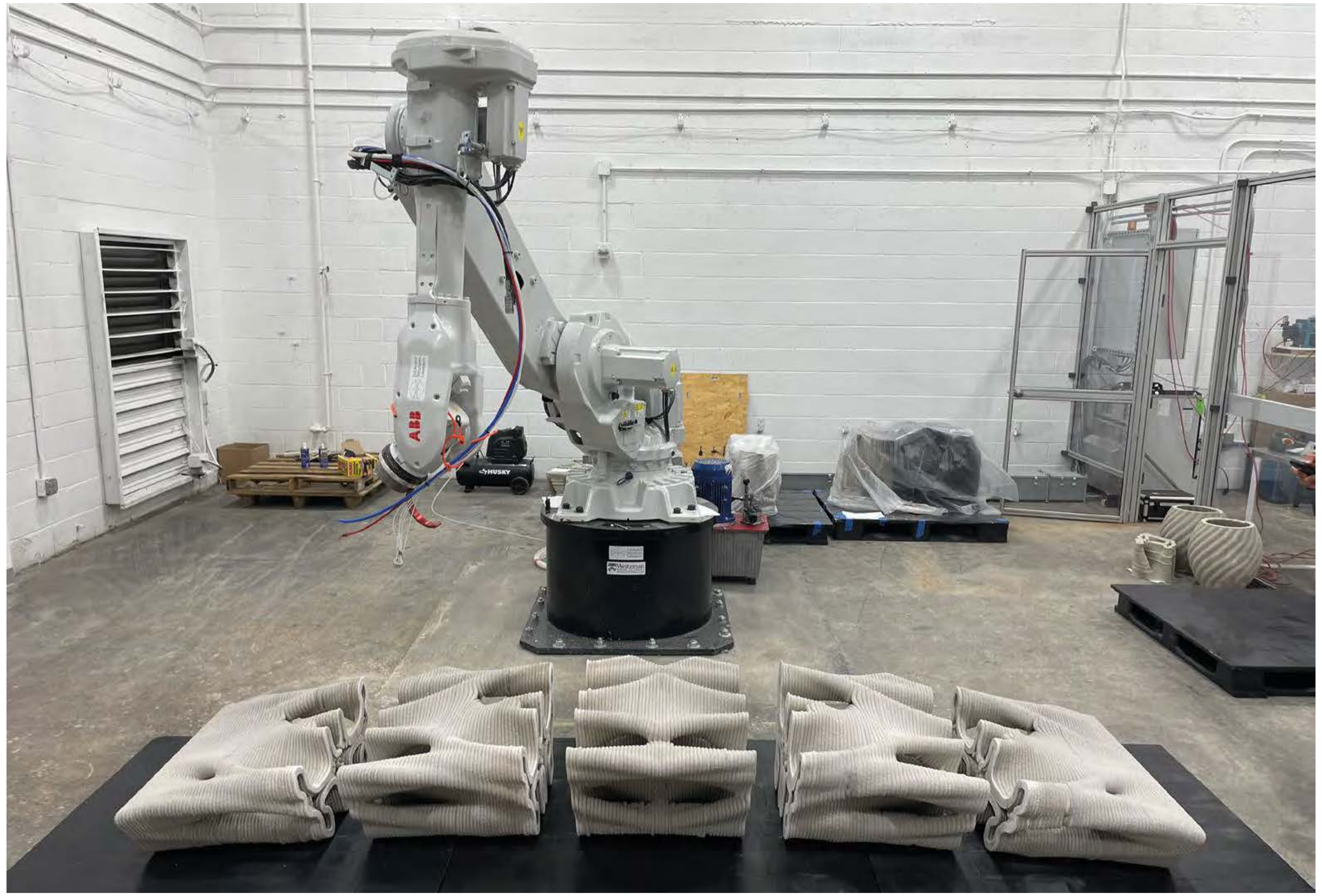

12

height of the jump. Finally, the contour was split at its closest point with the end of the current layer grouping and the start of the next layer of group. A connecting path linking those points to the split contour was created, giving one final path for each jump that can then be connected to the layers. For jumps with a duration of less than 2.5 seconds, a simple arc-shaped path was deemed sufficient. This optimisation, shown in Fig. 9, reduced potential printing issues and improved the quality and aesthetics of the part.

3D concrete printing and assembly

There are different technologies for 3D concrete printing available on the market, but the complexity of the canopy's design and the toolpathing needed indicated that a multi-component, accelerated system should be chosen for this project. The mix design incorporates three components, and follows this process: mortar powder is mixed with plasticiser and water in a continuous mixer, and then it is pumped to a high shear rate mixing printhead mounted on a robotic arm. At the printhead the mix is accelerated and extruded through the nozzle. The accelerator allows for a fast concrete setting time and higher overhang values. In comparison to one-component systems, where the height of the print is bound with a slower setting time of the layers that must withstand the load of the subsequent layers, an accelerated system allows for taller prints in one session with overall thinner walls. Nevertheless, the use of an accelerator with the concrete mix can influence its interlayer bonding strength. However, this issue has been accounted for in the canopy's design and through trial printing.

12. 3m concrete print of the canopy. © Polyhedral Structures Lab, University of Pennsylvania.

Another important aspect of 3D concrete printing is testing the material properties and using correct values for the finite element calculations. For regular cementitious systems, material properties such as compressive strength and flexural strength are measured using cast elements according to precise standards and methods. Unlike in regular cementitious systems, a widely accepted standard for 3D-printing applications does not exist, and while the mechanical properties of the concrete-mortar itself can also be measured on cast elements, it is already known that the presence of layers will affect their actual mechanical properties. Therefore, during the evaluation of the project, several adaptations of existing standards were made to best measure the influence of printed layers on the material properties. Then, the cast concrete properties were compared with the printed properties in different directions of the print to best understand the mechanics and characteristics of the material.

Through full-scale prototype printing, additional adjustments were made to the printing policy and toolpathing, as well as minor alternations to the design, to ensure successful fabrication. Between the prototyping and the larger-scale prints, an assembly strategy was developed. This strategy included how to best move, manipulate, and assemble the individual canopy segments for post-tensioning. An assembly sequence was developed using the small-scale prototype, whereby the canopy segments were placed on machined foam blocks with casters. Using a rail system, the individual pieces were placed together and post-tensioned (Fig. 11). Additional strategies for manipulating and placing the full-scale canopy for exhibition were implemented.

Closing remarks

The design, fabrication, and exhibition of *Diamanti canopy* demonstrates how the combination and development of new and existing methods and technologies can lead to high-performing composite structures with reduced material. The comprehensive computational methodology takes full advantage of the geometric capabilities of 3D concrete printing and directly addresses the unavoidable compression and tension forces developed in concrete structures by using post-tensioning. Overall, this project showcases how these technologies can be used for a more sustainable practice where high-performing structural systems can be produced and material recyclability can be achieved, reducing the overall carbon and embodied energy consumption.
The authors hope that this collaborative project inspires the AEC sector to implement and further develop the comprehensive design and fabrication workflow, thus expanding its use as a mainstream approach for exploring and producing forms that were previously impossible or uneconomical to build with conventional methods.

Acknowledgements

The authors gratefully acknowledge the support provided by the Advanced Research Projects Agency-Energy (ARPA-E) Grant of the U.S. Department of Energy (DE-AR0001631) to Dr Masoud Akbarzadeh. Also, this research was partially funded by the National Science Foundation CAREER Award (NSF CAREER-1944691 CMMI) and the National Science Foundation Future Eco Manufacturing Research Grant (NSF, FMRG-CMMI 2037097) awarded to Dr Masoud Akbarzadeh.

References

AASHTO. (2008) AASHTO LRFD bridge design specifications, American Association of State Highway and Transportation Officials, Washington, D.C.

Akbari, M., Lu, Y. and Akbarzadeh, M. (2021) From design to the fabrication of shellular funicular structures. In: Dörfler, K., Parascho, S., Scott, J., Bogosian, B., Farahi, B., Grant, J., García del Castillo y López, J.L. and Noel, V.A.A. eds., *ACADIA 2021 REALIGNMENTS: TOWARD CRITICAL COMPUTATION, Proceedings of the Association for Computer Aided Design in Architecture*. 3-6 November 2021, Online E-Conference, pp.328-339.

Akbarzadeh, M. (2016) 3D graphic statics using polyhedral reciprocal diagrams. Ph.D. thesis, ETH Zürich, Switzerland.

Bernhard, M., Bolhassani, M. and Akbarzadeh, M. (2021) Performative porosity – adaptive infills for concrete parts. In: *Proceedings of the IASS Annual Symposium 2020/21 and the 7th International Conference on Spatial Structures*. Surrey, UK, 23-27 August 2021.

Bernhard, M., Dillenburger, B. and Clemente, R. (2018) Axolotl. https://www.food4rhino.com/app/axolotl (Accessed: 10 January 2024).

Bernhard, M., Hansmeyer, M. and Dillenburger, B. (2018) Volumetric modelling for 3D printed architecture. In: Hesselgren, L., Kilian, A., Sorkine Hornung, O., Malek, S., Olsson, K-G. and Williams, C. J. K. eds., *AAG - Advances in Architectural Geometry*. Goteborg, Sweden: Klein Publishing GmbH, pp.392-415.

Blinn, J.F. (1982) A generalization of algebraic surface drawing. *ACM Transactions on Graphics*, 1(3), pp.235-256.

Lee, J. (2018) Computational design framework for 3D graphic statics. Ph.D. thesis, Zürich.

López López, D., Veenendaal, D., Akbarzadeh, M., Block, P. (2014) Prototype of an ultra-thin, concrete vaulted floor system. In: *Shells, Membranes and Spatial Structures: Footprints, Proceedings of the IASS-SLTE 2014 Symposium*. Brasilia, Brazil, 15-19 September 2014, pp.1-8.

Nuh, M., Oval, R., Orr, J. and Shepher, P. (2022) Digital fabrication of ribbed concrete shells using automated robotic concrete spraying. *Additive Manufacturing*, 59(B), p.103159.

Schwarz, H.A. (1865) *Ueber die minimalfläche, deren begrenzung als ein von vier kanten eines regulären tetraeders gebildetes räumliches vierseit gegeben ist*. Monatsberichte der Königlichen Akademie der Wissenschaften zu Berlin, pp.149-153.